Nat Immunol. Author manuscript; available in PMC 2016 August 03.

Published in final edited form as:

Nat Immunol. 2013 October ; 14(10): 1037–1044. doi:10.1038/ni.2692.

GATA-3 REGULATES THE SELF-RENEWAL OF LONG-TERM HEMATOPOIETIC STEM CELLS

Catherine Frelin[1,2], **Robert Herrington**[1], **Salima Janmohamed**[3], **Mary Barbara**[1], **Gary Tran**[1,2], **Christopher J. Paige**[1,2,3], **Patricia Benveniste**[3,5], **Juan-Carlos Zuñiga-Pflücker**[3,5], **Abdallah Souabni**[6], **Meinrad Busslinger**[6], and **Norman N Iscove**[1,2,3,4]

[1]Ontario Cancer Institute/UHN, Toronto, ON M5G 2M9, Canada

[2]Department of Medical Biophysics, University of Toronto, Toronto, ON M5S 1A8, Canada

[3]Department of Immunology, University of Toronto, Toronto, ON M5S 1A8, Canada

[4]McEwen Centre for Regenerative Medicine, Toronto, ON M5G 1L7, Canada

[5]Sunnybrook Research Institute, Toronto, ON M4N 3M5, Canada

[6]Research Institute of Molecular Pathology, Vienna, A-1030, Austria

Abstract

Gata3 is expressed and required for differentiation and function throughout the T lymphocyte lineage. Despite evidence it may also be expressed in multipotent hematopoietic stem cells (HSC), any role in these cells has remained unclear. Here we show GATA3 was cytoplasmic in quiescent long-term stem cells from steady state bone marrow, but relocated to the nucleus when HSC cycle. Relocation depended on p38-MAPK signaling and was associated with diminished capacity for long-term reconstitution upon transfer to irradiated mice. Deletion of Gata3 enhanced repopulating capacity and augmented self-renewal of long term HSC in cell-autonomous fashion, without affecting cell cycle. These observations position Gata3 as a regulator of the balance between self-renewal and differentiation in HSC acting downstream of the p38 signaling pathway.

GATA3 is a zinc finger transcription factor expressed and essential to differentiation and function throughout the T lymphocyte hierarchy [1]. In common with many transcription factors, its localization between cytoplasm and nucleus is governed by modification of its classical nuclear localization signal motif. In human T lymphocytes, the GATA3 nuclear localization motif is serine phosphorylated by activated p38/MAPK downstream of T cell receptor activation, leading to binding of importin α and carriage into the nucleus [8]. Besides expression in developing T cells, mRNA-level expression of *Gata3* has also been reported further upstream in sorted populations enriched for murine long-term multipotent

*Correspondence: iscove@uhnresearch.ca.

AUTHOR CONTRIBUTION

C. F. carried out most of the experimental work. The manuscript was written by C. F. and N. I. Some data elements were contributed by S. J., G. T., C. P., P. B. and J-C. Z-P. R. H. and M. B. provided technical support. A. S. and M. B. engineered and supplied the *Gata3* mutant mice and helped with the writing.

hemopoietic stem cells (LT-HSC) [2–4]. While the RNA evidence might indicate a functional role in HSC, it is puzzling that deletion of *Gata3* targeted to HSC has not yielded a hemopoietic deficiency phenotype outside the T lymphocyte lineage [5–7]. The absence of phenotype raises questions that remain outstanding, including whether *Gata3* transcripts were correctly attributed to LT-HSC as opposed to contaminating cell types in the impure HSC fractions analyzed, or whether RNA is translated in HSC to functional GATA3 protein. Further, as GATA3 depends on upstream signaling for its activation [8], it is not clear whether effects of deletion were fully tested in circumstances where GATA3 was in an active state.

HSC are capable of reconstituting all blood lineages from a single purified cell after transplant into irradiated mice [2,9]. Two distinct classes of HSC have recently been resolved based on differing biology and phenotypes. LT-HSC express SLAMF1 (CD150 antigen) [2,3,14] but not α_2 integrin (CD49b antigen) [2] and generate grafts that indefinitely sustain myeloid, erythroid and lymphoid cell output. They are deeply quiescent in the normal bone marrow steady state, with intermitotic intervals estimated at 50 – 100 d from histone H2B-GFP dilution rates [10,11]. Intermediate-term (IT-) HSC do express α_2 integrin [2] allowing their prospective separation from LT-HSC, are 3-fold more numerous [2,11] and generate systemic grafts from single injected cells which sustain myeloid and erythroid cell production for 12 wk before declining [2,3,12]. They are similarly quiescent in the normal steady-state, but reenter cycle more frequently (every 10 – 20 d) as evidenced by more rapid H2B-GFP dilution rates [10,11]. Their greater number, their extensive proliferative capacity and their more frequent exit from quiescence imply a dominant role in maintaining blood cell production in the steady-state [13]. *Gata3* transcripts are detected preferentially in α_2 integrin −ve fractions suggesting preferential expression in LT- rather than IT-HSC [2]. Given the known involvement of GATA3 in differentiation of progenitor hierarchies in T lymphocyte and mammary luminal epithelial lineages, the observation raised the intriguing possibility that GATA3 might be involved in specifying the sustained self-renewal property of LT-HSC or the transition from LT- to IT-HSC.

Here we report results that resolve the ambiguities in the earlier evidence and identify a novel role for GATA3 as an HSC-autonomous regulator of cell fate. Direct proof is provided for *Gata3* mRNA and protein expression in LT-HSC, but not more advanced HSC. Further, in LT-HSC purified to near functional homogeneity, GATA3 protein is shown to relocate from cytoplasm to nucleus in response to external signals, a change associated with both exit from quiescence and reduction in capacity for long-term reconstitution in irradiated hosts. Finally, we use conditional deletion of *Gata3* in LT-HSC to establish a causal link between GATA3 activation and reduction in long-term reconstitution activity, and thus to demonstrate gain in HSC self-renewal, without change in cycling parameters, as the essential deletion phenotype.

RESULTS

Gata3 RNA and protein are expressed in LT- but not IT-HSC

Quantitative RT-PCR confirmed that expression of *Gata3* transcripts in the Lineage^{lo}Sca-1^{+}c-Kit^{+}Rho^{lo}α_2Integrin^{lo} (LSKRα_2^{lo}) fraction, which contains LT-HSC at 30% functional purity[2], was 47-fold more abundent than in the LSKRα_2^{hi} fraction

consisting entirely of IT-HSC (Supplementary Fig. 1). To link *Gata3* expression more definitively to LT-HSC, we took advantage of a mouse strain (*Gata3*$^{GFP/+}$) in which exon 4 of the Gata3 gene is replaced with an eGFP cassette expressed from the endogenous *Gata3* promoter [15]. *Gata3*$^{GFP/+}$ bone marrow cells were sorted into eGFP negative, low and high fractions (Fig. 1a). Competitive 32 wk erythroid reconstitution assays (Fig. 1b) showed that all long-term reconstituting activity (as well as phenotypic LT-HSC; Supplementary Fig. 1) was present in the eGFP^{lo} and eGFP^{hi} fractions. In contrast, nearly all intermediate 8 – 16 wk activity remained in the eGFP^{-} fraction. These results indicate preferential transcriptional activity of *Gata3* genes in functionally defined LT-HSC.

Absence of a deletion phenotype might be expected if *Gata3* mRNA were not translated to functional protein in HSC. We therefore looked for GATA3 protein expression by immunostaining. GATA3 protein was detected in 30% of LSKRα_2^{lo} cells, which corresponds to the proportion of cells in this fraction able to generate long-term hemopoietic grafts [2], but was not detected in LSKRα_2^{hi} cells consisting entirely of IT-HSC (Fig. 2a,b). When SLAMF1 was added to the isolation strategy (Fig. 2c), 85% of LSKRα_2^{lo}SLAMF1^{hi} cells immunostained for GATA3 (Fig. 2e). In 32 wk erythroid reconstitution assays 50 LSKRα_2^{lo}SLAMF1^{hi} cells reproducibly competed 1:1 with 10^6 bone marrow cells (Figure 2D), which contain about 50 LT-HSC [2], suggesting essential functional homogeneity of this fraction. These observations showed direct correspondence between the proportion of cells immunostained for GATA3 protein and the extent of HSC purification, and suggested that the LSKRα_2^{lo}SLAMF1^{hi} marker combination achieves the closest approach to functional long-term HSC purification yet reported.

Localization of GATA3 protein responds to cellular signaling

Having established the presence of GATA3 protein in purified LT-HSC, we wanted to determine whether its behavior or activation state would be responsive to upstream signaling. GATA3 was cytoplasmic in quiescent, freshly isolated LSKRα_2^{lo} cells (Fig. 2a). To assess the responsiveness of GATA3 protein to cytokine signaling, LSKRα_2^{lo} cells were cultured with serum, Kit ligand, Flt3 ligand, Interleukin-11 (IL-11) and Interleukin-7 (IL-7). Cultured cells began dividing by 40 h [2]. GATA3 was readily detectable in cell nuclei by 24 h and was mainly nuclear by 48 h (Fig. 3a–c).

To determine whether nuclear entry of GATA3 might be controlled by p38, as in human T lymphocytes, we first asked whether p38 was activated in cultured LSKRα_2^{lo}SLAMF1^{hi} cells. Activation of p38α in cultured LSK cells was previously described [17]. However, LSKRα_2^{lo}SLAMF1^{hi} cells represent less than 3% of LSK cells and therefore activation of p38 specifically in LT-HSC expressing GATA3 remained to be established. As assessed by immunofluorescence microscopy, phospho-p38α was measurably elevated after 15 min exposure to medium containing serum and cytokines (Fig. 3d). To test directly for dependence of nuclear relocalization on activation by p38, we cultured HSC in the presence of specific inhibitors of p38α catalytic activity. Two agents were tested, SB203580, a “first generation” pyrimidinyl imidazole inhibitor [18], and SB239063, a “second generation” inhibitor of the same class with greater specificity for p38α and higher potency [19]. Both significantly inhibited nuclear localization of GATA3 at 10 μM (Fig. 3 e,f), within the

concentration range originally established for high p38α specificity [19,20]. Inhibition at 3 μM was more marked with SB239063. Neither inhibitor affected subsequent growth in culture (not shown). The observations show GATA3 protein translocates to the nucleus in LT-HSC following cytokine exposure and activation from quiescence, implicate activated p38 as a required signal for activation and nuclear entry of GATA3, and suggest a functional role for GATA3 in cycling as opposed to quiescent LT-HSC.

Poly(I:C) affects LT-HSC cycling, GATA3 localization and HSC performance

We next examined the functional consequences of *Gata3* deletion with a particular focus on regenerative activity following bone marrow transplantation, when HSC would be actively cycling. We deleted *Gata3* using an *Mx1-Cre* transgenic background, in which Cre expression is triggered in hemopoietic cells by type I interferons, typically induced by administration of poly(I:C), which signals thorugh Toll-like receptor 3 to induce multiple downstream effects in addition to type I interferon expression [21]. Because of the likelihood that poly(I:C) administration might itself affect HSC independent of *Gata3* deletion, we first characterized its effects on HSC in wild-type mice. Poly(I:C) is known to induce HSC cycling *in vivo*, with a single injection having maximal effect at 48h followed by return to quiescence by 4 d [22]. We analysed the in vivo cell cycle response of LSKα_2^{lo}SLAMF1^{hi} cells one and ten days after 3 successive poly(I:C) injections, omitting the Rhodamine123^{lo} marker because it is selective for quiescent cells. Freshly isolated cells were stained intracellularly with Ki67 and Hoechst 33342 (Fig. 4a). Most (81%) LSKα_2^{lo}SLAMF1^{hi} cells were in G1 or G2/M one day after poly(I:C) and returned to quiescence by ten days. We also examined GATA3 protein localization in these cells on day 1, 10 and 5 months after poly(I:C) injection (Fig. 4b). GATA3 was still mostly nuclear at 10 d, but 5 months after treatment a substantial proportion of GATA3 was again cytoplasmic. Thus, as observed *in vitro*, relocation of GATA3 to the nucleus of HSC also occurred *in vivo* after treatment that induced HSC cycling, and was followed by delayed return to the cytoplasm after reversion of HSC to quiescence.

We next asked whether nuclear relocated GATA3 might affect the regenerative activity of LT-HSC. Following treatment of wild-type mice with poly(I:C), bone marrow LSKRα_2^{lo} cells were isolated 10 days or 5 months later and transplanted into irradiated hosts in competition with unfractionated wild-type recipient-genotype bone marrow cells. At 8 wk after transplantation, cells obtained at either timepoint after poly(I:C) treatment achieved similar levels of erythroid reconstitution to cells from untreated mice (Fig. 4c), suggesting that IT-HSC (normally the majority HSC type in the LSKRα_2^{lo} fraction [2]) were not affected. However, 24 – 32 weeks after transplantation, LSKRα_2^{lo} cells that had been treated with poly(I:C) 10 days before transplantation - when the cells had returned to quiescence but in which GATA3 was still intranuclear - yielded markedly lower levels of erythroid reconstitution (Fig. 4c) which represented a 6-fold reduction in number of long-term reconstituting cells by poly(I:C) treatment. This result was concordant with earlier reports of a depleting effect of poly(I:C) treatment on the long-term reconstituting potential of bone marrow cells [22,23]. In contrast, robust reconstitutions were achieved by either non-poly(I:C) treated control cells or LSKRα_2^{lo} cells treated with poly(I:C) 5 months previous to transplantation (Fig. 4c), in which GATA3 was again cytoplasmic (Fig. 4b). These

observations indicate that HSC containing nuclear GATA3 had diminished long-term reconstituting capacity, suggesting a correlation between LT-HSC regenerative performance and localization of GATA3, while regenerative activity of IT-HSC, which lack GATA3, was close to control levels after poly(I:C) treatment.

Gata3 deletion has little effect on steady-state hemopoiesis

For deletion of Gata3 in hemopoietic cells we used a mouse strain (*Gata3*$^{fl/fl}$) in which the 4th exon of Gata3 encoding the first zinc finger is flanked by LoxP sequences [24]. *Gata3*$^{fl/fl}$ mice were crossed with *Mx1-Cre* mice to yield *Gata3*$^{fl/fl}$-*Mx1-Cre* mice. Induction of Cre recombinase in these mice yields a truncated *Gata3* transcript predicted to splice out-of-frame to exon 5 containing the second zinc finger, translating to an inactive protein lacking both zinc fingers [24]. *Gata3*$^{fl/fl}$ mice that received the same poly(I:C) treatment as *Gata3*$^{fl/fl}$-*Mx1-Cre* mice were routinely used as undeleted controls.

Gata3$^{fl/fl}$-*Mx1-Cre* mice were treated with poly(I:C) to induce deletion of *Gata3*, and blood cells and bone marrow precursor populations were examined 3 – 9 mo later. Little effect of *Gata3* excision was evident either on the proportions (Fig. 5a) or absolute numbers (not shown) of circulating myeloid or lymphoid cells or on the number of LSKRα_2^{lo}SLAMF1^{hi} and LSKRα_2^{hi}SLAMF1^{lo} HSC in the bone marrow. Because a previous report had suggested that *Gata3*-deficient HSC were more quiescent in steady state conditions than intact HSC [7], we also examined the cell cycle status of LSKα_2^{lo}SLAMF1^{hi} cells by Ki67/Hoechst 33342 intracellular staining in the bone marrow of *Gata3*$^{fl/fl}$-*Mx1-Cre* and *Gata3*$^{fl/fl}$ mice 3 mo after treatment with poly(I:C). 85% of LSKα_2^{lo}SLAMF1^{hi} cells were quiescent, with no significant difference in Ki67/Hoechst staining distributions between undeleted *Gata3*$^{fl/fl}$ control or *Gata3*$^{fl/fl}$-*Mx1-Cre* mice (Fig. 5b). We also tested the cell cycle response of *Gata3*-deficient LSKα_2^{lo}SLAMF1^{hi} cells to a second round of poly(I:C) treatment and found they entered cell cycle to a similar degree as *Gata3*-intact controls (Fig. 5b). The lack of apparent effect of *Gata3* deletion on steady state bone marrow maintenance confirms an earlier report [6] and is consistent with the cytoplasmic localization of GATA3 protein in quiescent LT-HSC. Diagnostic PCRs on total bone marrow cells and circulating myeloid cells at various times after 3 successive poly(I:C) injections regularly indicated a minimum 97% efficiency of *Gata3* excision (Fig. 5c). Additionally, in clones grown in culture from individual LSKR cells obtained 10 d following poly(I:C) treatment, *Gata3* excision was complete in 99 of 101 the clones examined. These results showed that *Gata3* deficiency had little effect on blood cell production or LT-HSC maintenance in steady-state conditions where LT-HSC were quiescent and where GATA3 was mainly cytoplasmic.

Gata3 excision protects LT-HSC from depletion by poly(I:C)

We next looked for possible consequences of *Gata3* deficiency in conditions where GATA3 would be intranuclear. Unfractionated bone marrow cells, 10^6, from *Gata3*$^{fl/fl}$-*Mx1-Cre* or *Gata3*$^{fl/fl}$ mice 10 days after poly(I:C) treatment - when GATA3 was mainly nuclear (Fig. 4b) -were each injected in competition with 10^6 untreated wild-type bone marrow cells into irradiated recipients. Hematopoietic reconstitution in primary transplant recipients was tracked at 8, 16, 24 and 32 weeks as a measure of the long-term reconstitution potential of transferred cells. While long-term reconstituting activity was depleted in poly(I:C)-treated

wild-type bone marrow, no defect was seen with poly(I:C)-treated *Gata3*$^{fl/fl}$-*Mx1-Cre* bone marrow which robustly sustained erythroid, myeloid and B lymphocytic lineages in primary recipients up to 32 weeks (Fig. 6a), matching or exceeding the regenerative activity of the co-injected untreated wild-type competitor cells. As expected, T lymphocyte regeneration from poly(I:C)-treated *Gata3*$^{fl/fl}$-*Mx1-Cre* bone marrow was weak relative to myeloid and B lymphocyte reconstitution (Fig. 6a). These results showed that poly(I:C)-induced nuclear translocation of GATA3 impaired the long-term regenerative capacity of bone marrow LT-HSC and that deletion of the *Gata3* gene reversed the effect.

Gata-3 deletion enhances LT-HSC expansion *in vivo*

Because GATA3 relocated to the nucleus when LT-HSCs were induced to cycle, we next asked whether functional consequences of *Gata3* deletion might be apparent in LT-HSC after transfer into irradiated mice, where they enter active cell cycle and have been shown to expand in number by a factor of 10 after transplantation of 10^6 bone marrow cells [25,26]. *Gata3*$^{fl/fl}$-*Mx1-Cre* mice were treated with poly(I:C) to delete *Gata3*. Bone marrow was taken 10 d later and erythroid regenerative activity was measured competitively in primary recipient mice by coinjection of 10^6 unfractionated cells with the same number of bone marrow cells from untreated wild-type mice of recipient genotype. The proportions of donor and competitor erythrocytes were measured in blood at 24 wk by GPI1 assay #1, from which numbers of Gata3-deleted LT-HSC initially injected were estimated as in [2].

Unfractionated bone marrow obtained at 24 wk from 1° recipients was transplanted into irradiated 2° recipients. After a further 24 wk, proportions of donor and competitor erythrocytes were again determined in GPI1 assay #2, and unfractionated bone marrow from 2° recipients was injected in varying numbers into 3° recipients for enumeration of LT-HSC originating from Gata3-deleted and wild-type competitors by limiting dilution of 20 wk erythroid reconstituting activity. Results of GPI1 assay #2, the limiting dilution assay and the historically determined content of 10^6 normal competitors were combined as in [2] to yield the numbers of LT-HSC initially injected into secondary recipients and the number recovered from them. These numbers were used to compute the net numerical expansions of LT-HSC occuring in primary and secondary recipients (Fig 6b). Untreated wild-type competitor HSCs expanded in primary and secondary recipients by 10- and 7.5-fold in number during the primary and secondary reconstitution respectively to achieve a cumulative expansion of 75-fold. In contrast, *Gata3*-deficient LT-HSC expanded by 20-fold during regeneration in primary recipient mice and a further 13-fold in secondary recipients to achieve a cumulative 260-fold increase over the number of initially transferred cells (Fig. 6b). These results showed that *Gata3*-deficient LT-HSC expanded to a greater extent during sequential regeneration *in vivo* than wild-type control HSC, suggesting that GATA3 must restrain the extent to which normal LT-HSC expand during bone marrow regeneration.

GATA3 effects on HSC self-renewal are HSC-autonomous

To ensure that the regenerative advantage of *Gata3*-deficient HSCs was HSC-autonomous, and not due to systemic effects of *Gata3* deletion in the poly(I:C)-treated *Gata3*$^{fl/fl}$-*Mx1-Cre* mice, we transplanted 0.5 x 10^6 unfractionated *Gata3*$^{fl/fl}$-*Mx1-Cre* or *Gata3*$^{fl/fl}$ bone marrow cells together with 10^6 wild-type control bone marrow cells into irradiated wild-type mice

and induced *Gata3* deletion with poly(I:C) treatment 8 wk post-transfer. In this experimental strategy *Gata3* would be deleted only in the regenerated *Gata3*$^{fl/fl}$-*Mx1-Cre* cells. 24 wk after reconstitution, unfractionated bone marrow cells from the mixed chimeras were injected into secondary irradiated hosts and the extent of erythroid regeneration from *Gata3*-deleted versus control competitor cells was quantified. *Gata3*-deficient bone marrow cells again had a marked erythroid regenerative advantage compared to wild-type cells (Fig. 6c). These results suggest a cell-autonomous effect of *Gata3* on the regenerative advantage of HSCs, independent of the environment in which deletion was induced.

Gata3 excision protects LT-HSC from depletion in culture

We also tested the functional consequences of *Gata3* deletion in cultured LT-HSC, in which GATA3 also relocates to the nucleus (Fig. 3). Purified, quiescent LSKRα_2^{lo} or LSKRα2^{lo}SLAMF1^{hi} cells isolated from *Gata3*$^{fl/fl}$-*Mx1-Cre* mice treated with poly(I:C) 3 – 5 months before isolation or from wild-type untreated mice were cultured for 7 days. During culture, neither the cloning efficiency (90 – 95%), the latency to onset of growth[2] (not shown), cell numbers nor subsequent division rate (Fig. 6d) were significantly affected by *Gata3* deletion in comparison with wild-type controls. Purified wild-type LT-HSC normally maintain their *in vivo* competitive reconstituting activity for the first 4 d in culture. Activity falls off steeply thereafter and little or no long-term activity is recovered by 7 d (Fig. 6e). In contrast, *Gata3*-deficient HSCs maintained their long-term competititve reconstituting activity throughout the 7 days of culture. These results add to the evidence that activated GATA3 exerts a negative regulatory action on the long-term regenerative capacity of LT-HSC, in a way unlikely to involve changes in cell cycling.

DISCUSSION

Earlier work has suggested that GATA3 has little impact on steady-state hemopoiesis beyond its role in T lymphocyte production and function [5–7]. Here we report novel observations that explain the earlier results and define a strong functional role for GATA3 in LT-HSC. The quiescence of LT-HSC and sequestration of GATA3 to the cytoplasm in steady state bone marrow provide a plausible basis for the observations, here and earlier, demonstrating little effect of *Gata3* deletion on steady-state hemopoiesis: most GATA3 protein is inactive in quiescent LT-HSC and its deletion should not influence their behavior, while IT-HSC which perform the bulk of bone marrow maintenance do not express *Gata3*. Deficiency of *Gata3* in regenerative contexts did not lead to loss of function, which earlier studies were configured to detect, but rather gain in extent of self-renewal, whose detection requires suitably configured quantitative assays. In every context tested - growth in culture, response to poly(I:C) *in vivo* and regeneration following transfer into irradiated mice - deletion of *Gata3* led to enhancement in numbers of LT-HSC detected in functional assays. Moreover, the experiments measuring expansion *in vivo* showed that the effects of *Gata3* deletion were LT-HSC-autonomous. Thus, deletion of *Gata3* consistently led to gain in self-renewal during LT-HSC proliferation, suggesting a role for GATA3 in restraining self-renewal in proliferating LT-HSC.

Although our findings confirm a lack of effect of *Gata3* deletion on steady state bone marrow function as documented earlier [6], the marked enhancement of LT-HSC self-renewal documented here in irradiated hosts was not apparent in the earlier study. Differing *Gata3* deletion strategies could account for the discrepancy. The previous study [6] used a Vav-Cre background to achieve *Gata3* excision at first emergence of HSC from hemogenic endothelium in the embryo. It is possible that homeostatic adjustments in expression of compensatory genes were more complete in that model than in our Mx1-Cre model that deleted *Gata3* in adult life in already formed LT-HSC.

The means by which GATA3 restrains self-renewal remain to be determined. One possible mechanism would be restraint of proliferation. Such an effect would be contrary to studies suggesting that GATA3 actually promotes cycling of LT-HSC [7]. However, we did not observe any effects of *Gata3* deletion on cell cycle either *in vitro* or *in vivo*. Promotion of apoptosis in cycling cells is another formal possibility but was similarly not supported by our kinetic observations in culture. An attractive alternative mechanism would be promotion of differentiation of LT-HSC toward IT-HSC, a step that we show here also involves sharp down-regulation of *Gata3*. Such a role would place GATA3 as a regulator of the balance between self-renewal and differentiation in LT-HSC, mediating their reprogramming from a multipotent cell with unlimited regenerative lifetime to a multipotent IT-HSC with a 3 month regenerative potential.

An analogous “pro-differentiation” role for GATA3 has been shown in luminal breast epithelial progenitors, where GATA3 is required for differentiation to a mature ductal epithelial phenotype and where its deletion results in numerical expansion of undifferentiated precursors [27]. While in luminal stem cells the GATA3 requirement for differentiation appears absolute, LT-HSC are still able to differentiate in its absence, suggesting redundancy in elements controlling the differentiation process [6]. In the mammary system, GATA3 collaborates with FOXA1 as a “pioneer” factor [28–31] involved in nucleating a remodelling complex at heterochromatic estrogen receptor target regions that leads to opening and epigenetic marking of the sites for active transcription. A similar role in LT-HSC could provide a mechanism for stable transformation of cellular identity to the IT-HSC stage.

If GATA3 suppresses self-renewal in proliferating LT-HSC, an apparent paradox arises: when bone marrow is transplanted into irradiated recipient mice, the number of LT-HSC normally increases 10-fold over the number injected in the weeks following the transplant [9,25,26]. LT-HSC are induced to proliferate in bone marrow-ablated milieus [32,33], and GATA3 might be expected to be activated and relocate to the nucleus. If so, how would a net increase in LT-HSC occur? We were unable to assess the extent of nuclear entry of GATA3 by immunofluorescence microscopy in this setting because marker sets that allow purification to homogeneity of quiescent LT-HSC do not yield sufficient functional purity when applied to regenerating bone marrow [34]. Conceivably, the degree of GATA3 activation and nuclear relocation in physiologically regenerating bone marrow could be less than what we observed in culture or *in vivo* consequent to treatment with poly(I:C). Positive signals may also be available in regenerating bone marrow which partially balance out the negative action of GATA3. Nevertheless, deletion of *Gata3* augmented expansion of LT-HSCs injected,

suggesting that in physiologically regenerating bone marrow GATA3 is activated at a level sufficient to constrain, but not to abolish, increases in LT-HSC numbers.

Translocation of GATA3 to the nucleus was shown in human T lymphocytes to depend on serine phosphorylation at the nuclear localization signal sequence via direct catalysis by p38 and consequent interaction with importin-α [8]. To test for corresponding p38α dependence in LT-HSC, we used two selective p38α inhibitors whose few known off-target kinases are affected only at concentrations 1 – 2 orders of magnitude higher than those used here [19,20,35,36]. Our results in murine LT-HSC confirm in a new cellular context that activation of GATA3 depends on activated p38. Crucially, we also confirmed that p38α is indeed activated in cultured LT-HSC. Activation of p38α has also been documented downstream of TLR3 receptors responding to poly(I:C) in dendritic and NK cells [37,38], as well as c-kit [39], TNF and LTα [40] and reactive oxygen signaling [41] in a variety of hemopoietic cells. Our identification of GATA3 as a negative agonist in LT-HSC responding to the activation state of the p38 signaling pathway implicates it as a potentially critical mediator of the LT-HSC-depleting effects of inflammatory cytokines and reactive oxygen in the earliest hemopoietic stem cells. These effects should be mitigated by inhibition of p38 signaling, and enhanced preservation of LT-HSC cultured in the presence of p38α inhibitors has indeed been observed [17]. Our findings collectively identify a physiological mechanism that constrains the capacity of bone marrow stem cells to engraft long-term, and show that interference with that mechanism can lead to enhanced self-renewal of LT-HSC. The observations have important potential implications for enhancing stem cell expansion both in culture and in vivo.

METHODS

Mice

Gata3$^{GFP/+}$ and *Gata3*$^{fl/fl}$ mice were maintained by M.B. [15,24] and backcrossed to C57BL/6J mice for 5 or more generations before use. The genotyping primers for *Gata3*$^{GFP/+}$mice were: 5′-CGCCGCCGGGATCACTCTCG-3′ and 5′-GATCCAGACATGATAAGATACA-3′. *Gata3*$^{fl/fl}$ mice were bred with C57BL/6J-Mx1-cre deleter mice obtained from The Jackson laborarory, Bar Harbor, ME. The genotyping primers for Cre were 5′-GCGGTCTGGCAGTAAAAACTATC-3′ and 5′-GTGAAACAGCATTGC TGTCACTT-3′, and for *Gata3* fl and WT alleles 5′-GTCAGGGCACTAAGGGTTGTT-3′ and 5′-TGGTAGAGTCCGCAGGCATTG-3′. Excision of the *Gata3*^{fl} allele was detected using 5′-GTCAGGGCACTAAGGGTTGTT-3′ and 5′-TATCAGCGGTTCATCTACAGC-3′.

Bone marrow donor genotypes were C57BL/6J-Ly5.2-Gpi1$^{b/b}$, C57BL/6J-*Gata3*$^{GFP/+}$-Ly5.2-Gpi1$^{b/b}$, C57BL/6J-*Gata3*$^{fl/fl}$-Ly5.2-Gpi1$^{b/b}$, and C57BL/6J-*Mx1-cre*-*Gata3*$^{fl/fl}$Ly5.2-Gpi1$^{b/b}$. Recipient mice were C57BL/6J-Ly5.1-Gpi1$^{a/a}$. HSC purifications were performed on bone marrow from mice that were at least 16 wk old. Animal experiments were conducted under the ethical oversight of the Animal Care Committee of the Ontario Cancer Institute.

For excision of *Gata3* in *Gata3*$^{fl/fl}$-*Mx1-Cre*$^{+}$ mice, 300 μg high MW poly(I:C) (InvivoGen, San Diego, CA) in isotonic saline was administered intraperitoneally on alternate days for a total of 3 injections. Mice did not exhibit adverse effects of treatment.

Cell Culture

Cells were incubated at 37°C in 5% CO_2 in U-bottom microtiter wells (Nunclon) in 100 μl IMDM containing 7.5 x 10^{-5} M α-thioglycerol, 4% FBS, 0.1% BSA, 5 μg/ml transferrin, 5 μg/ml insulin, 50 ng/ml c-kit ligand (KL), 50 ng/ml Flt3 ligand (FL), 10 ng/ml interleukin-11 (IL-11), and IL-7 conditioned medium all as detailed in [2,9]. For growth kinetics of single cells, sorted cells were plated at limiting dilution and wells containing exactly 1 cell were identified visually after 18 hr culture.

p38 MAPK inhibitors

The inhibitors SB239063 and SB203580 (Sigma-Aldrich) were dissolved in DMSO at 10 mM concentration. The final concentration of DMSO added to the cultures was 0.03 – 0.1% v/v. Control cultures contained the same amounts of DMSO only. No effect on growth was seen at these concentrations of inhibitor or solvent.

Reconstitution Assays

Quantitative competitive assays were performed by coinjecting C57BL/6J-Ly5.2-Gpi1$^{b/b}$ bone marrow cells or 30 to 100 purified HSC with 0.5 – 1 x 10^6 C57BL/6J-Ly5.1-Gpi1$^{a/a}$ bone marrow competitors into irradiated (9 Gy, Cs^{137}) C57BL/6J-Ly5.1-Gpi1$^{a/a}$ mice. Limiting dilution assays were performed in sublethally irradiated (4 Gy, Cs^{137}) C57BL/6J-Ly5.1-Kit$^{W\text{-}41J/W\text{-}41J}$-Gpi1$^{a/a}$ hosts. The ratio [(proportion donor) / (1 – proportion donor)] is linearly related to the number of HSC injected in competitive assays [42]. This value was combined with the known frequency of LT-HSC in normal competitor bone marrow (1:18200, [2]) to derive from competitive assay outcomes, typically erythroid reconstitution values, an estimate of the absolute numbers of HSC in the assayed samples as detailed in [2,26].

For the experiment shown in Fig 6b, *Gata3*-deleted bone marrow cells, 10^6, were transplanted into irradiated 1° recipients with 10^6 normal competitors. The proportions of donor and competitor erythrocytes were measured in blood at 24 wk, followed by transplant of 1.5 x 10^7 1° bone marrow cells without fresh competitors into irradiated 2° recipients. Proportions of donor and competitor erythrocytes were measured at 24 wk. Erythroid reconstituting cells in bone marrow from 2° recipients were enumerated by limiting dilution analysis. 4 Gy irradiated B6-Kit$^{W–41J/W–41J}$ mice were transplanted with 2, 6 or 8 x 10^5 cells per mouse followed by enumeration of mice positive for erythroid reconstitution at 20 wk. Mice had either undetectable reconstitution or at least 15% donor erythrocytes.

For the experiment shown in Fig. 6c, ^{5} x 10^2 *Gata3*$^{fl/fl}$ or *Gata3*$^{fl/fl}$-*Mx1-Cre*$^{+}$ bone marrow cells were injected with 10^6 normal competitors into irradiated wild type recipients. Hosts were treated with poly(I:C) 8 wk later. The proportion of donor erythrocytes in blood was measured at 24 wk and was used to estimate the number of LT-HSC that were originally injected. Host bone marrow cells, 1.5 x 10^7, were subsequently passaged to irradiated

recipients and proportions of donor erythrocytes were determined after 20 wk. These values were used to estimate the number of LT-HSC regenerated in the 1° recipients. The bar graph shows the fold-expansion in LT-HSC numbers calculated to have occurred in the 1° recipients with SEMs indicated (single experiment, 3 – 5 mice per point, * = .04, 1-tail T test).

For the experiment shown in Fig. 6d, bone marrow from *Gata3*$^{fl/fl}$-*Mx1-Cre*^{I} and control *Gata3*$^{fl/fl}$ mice was analyzed 2–3 months after treatment with poly(I:C). Single LSKRα_2^{lo} (n=3 independent experiments) or LSKRα_2^{lo}SLAMF1^{hi} (n=1) cells were cultured in microwells with serum and cytokines, and the number of cells per well was recorded every 4–8 hr. 30 clones from each HSC fraction were tracked. Each point represents the sum of cells in 30 wells.

For the experiment shown in Fig. 6e, *Gata3*$^{fl/fl}$-*Mx1-Cre* and control *Gata3*$^{fl/fl}$ mice were sacrificed 3 – 5 months after treatment with poly(I:C). LSKRα_2^{lo}SLAMF1^{hi} cells, 25, were cultured at 1 per 100 μl well in medium containing serum and cytokines, and also coinjected with 0.5 x 10^6 host-genotype competitor cells into each irradiated recipient in order to measure the amount of long-term reconstituting activity initially placed into culture. After culture for 7 d, all harvested cells were injected with 0.5 x 10^6 competitors into each irradiated recipient. Erythroid reconstitution was measured at 32 wk.

Detection of Donor Erythrocytes, Myeloid and Lymphoid Cells

Erythrocyte Gpi1 isoforms were resolved by flat bed electrophoresis on Super Sepraphore membranes (cellulose acetate on Mylar, VWR/Pall) and Gpi1 bands quantitated as described [2]. For leukocytes, erythrocytes were lysed in NH_4Cl, Fc receptors were blocked with anti-CD16/32 antibody (eBioscience, clone 93) followed by reaction with fluorochrome-conjugated anti-Ly5.1 (eBioscience clone A20), anti-Ly5.2 (eBioscience clone 104), anti-B220 (eBiosciences clone RA36B2), anti-CD11b (eBioscience clone M1/70), anti-Ly6Gr1 (eBioscience clone RB6-8C5) and anti-TCRβ (eBioscience clone H57-597) antibodies. Labelled cells were analysed by flow cytometry (LSRII, Beckton-Dickinson, Mountain view, CA, USA). The proportion of donor cells was expressed as proportion donor within the stated lineage.

Purification of HSC

Femoral and tibial bone marrow cells were treated with NH_4Cl for lysis of red cells, stained/destained with Rhodamine123 (Eastman Kodak), incubated with Fc receptor blocking antibody for 5 min (anti-CD16/32, eBioscience, clone 93) and then with PE-Cy5-conjugated anti-B220 (eBioscience, clone RA3-6B2) and anti-CD3 (eBioscience, clone 145-2C11) for 30 min at 4°C as detailed in [2]. Washed cells were separated on a ARIA (BD) sorter and the Rho^{lo}B220^{-}CD3^{-} fraction collected. Recovered cells were labeled with fluorochrome-conjugated PE-anti-CD49b (BD Pharmingen, clone HMα2), PE-Cy7-anti-c-kit (eBioscience, clone 2B8), and APC-anti-Sca-1 (eBioscience, clone D7) antibodies for 30 min, washed and sorted for LSKRα_2 integrin low and high cells. For isolations using both α_2 integrin and CD150 markers, cells after Rhodamine123 staining/destaining were lineage depleted (CD5, B220, CD11b, Gr1, 7/4 and Ter-119) using magnetic beads and an

Automacs separator (Miltenyi Biotec, BergischGladbach, Germany)). Lineage depleted cells were incubated with Fc receptor blocking antibody and then stained with PE-Cy5-anti Streptavidin (eBioscience), PE-Cy5 anti-CD3 (eBioscience, clone 145-2C11), PE-Cy7-anti-c-kit, APC-anti-Sca-1, Pacific-Blue-anti-CD150 (Biolegend clone TC15-12F12.2) and PE-anti-CD49b antibodies for 30 min, washed and sorted.

Transcript Expression in Purified Cells

Globally amplified cDNAs from LSKR-α_2^{lo} and -α_2^{hi} cells were described in [2]. cDNAs from the erythromyeloid hierarchy were described in [43,44]. RNA from purified stages in the B [45] and T lymphocyte [46] hierarchies was globally amplified as described in [47]. PCR primers targeting sequence within a 300 bp range upstream of polyadenylation sites [48] were used for detection of specific transcripts in amplified cDNA. Primers for *Gata3* were: 5′-GTCACTTTTCTTGCAGCCTA-3′ and 5′-CAGACTGTTTAAAGGCAGTG-3′. *Gata3* transcript expression was analysed by Q-RT-PCR using the QuantiTect SYBR Green PCR Kit (Qiagen, Hilden, Germany) on an ABI 7900HT Fast Real-Time PCR system (Applied Biosystems, California USA).Ct (threshold cycle) values were normalized to the endogenous control gene GAPDH ($\Delta CT = Ct_{target} - Ctendogenous$) and compared to the mean of the LSKR$\alpha_2^{hi}\Delta CT$ calibrator using the $\Delta\Delta CT$ method ($\Delta\Delta CT = \Delta CT_{sample} - \Delta CT_{calibrator}$).

Immunofluorescence and Confocal Analysis

Freshly sorted cells, typically 100–200, were dropped on polylysine coated slides in a humid chamber at room temperature for 30 min followed by fixation for 10 min in PBS 2% fomaldehyde, permeabilization for 10 min in PBS/0.2% TritonX and blocking for 20 min in PBS containing 10% goat serum. Fixed and permeabilized cells were stained for 1h at room temperature with a mouse anti-human GATA3 antibody (HG3-31, IgG, Santa Cruz Biotechnology, or mouse IgG control (Santa Cruz Biotechnology) followed by labeling with Alexa Fluor 555-conjugated goat anti-mouse IgG antibodies for 45 minutes at room temperature in the dark. Slides were mounted with mowiol 4–88 medium (Calbiochem-Merck Chemicals, Darmstadt, Germany) containing DAPI. Cells were imaged by conventional (Zeiss AxioImager) or confocal (Zeiss LSM700) fluorescence microscopy. Fluorescence signal was quantified in individual cell images using ImageJ (http://rsb.info.nih.gov/ij/index.html).

For phospho-p38 MAPK staining, LT-HSC were sorted and cultured for 1 h at 37°C in IMDM without cytokines and serum followed by a 15 min pulse in IMDM containing 4% FBS, 0.1% BSA, 5 μg/ml transferrin, 5 μg/ml insulin, 50 ng/ml c-kit ligand (KL), 50 ng/ml Flt3 ligand (FL), 10 ng/ml interleukin-11 (IL-11), and IL-7. Cells were then fixed for 10 min in PBS/2% formaldehyde, permeabilized for 10 min in PBS/0.2% TritonX, blocked in PBS containing 10% goat serum for 20 min and stained with anti-phospho-p38 MAPK AlexaFluor 555 conjugated antibody (Cell signaling technology, clone D3F9) for 1 h.

DNA purification

2 to 10 x 10^6 bone marrow or peripheral blood cells were lysed in 0.2 to 1 ml DNAzol lysis buffer (Invitrogen), gDNA was precipitated using 100 to 500 μl EtOH 100%, washed twice

with EtOH 70% and diluted into H_2O. *Gata3* excision was assessed by semi-quantitative PCR.

Cell cycle analysis

Bone marrow cells were lineage depleted using magnetic beads and an Automacs separator (Miltenyi Biotec, Bergisch Gladbach, Germany) followed by labeling with APC-efluor780-anti-Streptavidin (eBiosciences), PE-Cy7-anti-c-kit, APC-anti-Sca-1, PEcy5-anti-CD150 (Biolegend clone TC15-12F12.2) and PE-anti-CD49b antibodies for 30 min followed by fixation and permeabilization in cytofix/cytoperm buffer (BD Pharmingen, Franklin Lakes, NJ, USA). After fixation/permeabilization, cells were stained with anti-human Ki67 antibody (BD Pharmingen, clone B56) for 20 minutes and Hoechst 33342 at 20 μg/ml (Molecular probes) for 5 minutes. Labelled cells were analysed by flow cytometry (LSRII, Beckton-Dickinson, Mountain view, CA, USA).

Supplementary Material

Refer to Web version on PubMed Central for supplementary material.

Acknowledgments

We thank P. A. Penttilä for assistance with flow cytometry and M.F. Monroy for help with animal procedures. The work was funded by grants from the Terry Fox Foundation, the Canadian Cancer Research Institute, the Canadian Institutes of Health Research, the Stem Cell Network. CF received fellowship support from the Fondation de France and the Fondation pour la Recherche Médicale. Additional support came from the McEwen Centre for Regenerative Medicine, the Princess Margaret Hospital Foundation, and the Campbell Family Institute for Cancer Research. This research was funded in part by the Ontario Ministry of Health and Long Term Care. The views expressed do not necessarily reflect those of the OMOHLTC.

References

1. Ho IC, Tai TS, Pai SY. GATA3 and the T-cell lineage: essential functions before and after T-helper-2-cell differentiation. Nat Rev Immunol. 2009; 9:125–35. [PubMed: 19151747]
2. Benveniste P, et al. Intermediate-term hematopoietic stem cells with extended but time-limited reconstitution potential. Cell Stem Cell. 2010; 6:48–58. [PubMed: 20074534]
3. Kent DG, et al. Prospective isolation and molecular characterization of hematopoietic stem cells with durable self-renewal potential. Blood. 2009; 113:6342–6350. [PubMed: 19377048]
4. Zhong JF, et al. Gene expression profile of murine long-term reconstituting vs. short-term reconstituting hematopoietic stem cells. Proc Natl Acad Sci U S A. 2005; 102:2448–53. [PubMed: 15695585]
5. Hosoya T, et al. GATA-3 is required for early T lineage progenitor development. J Exp Med. 2009; 206:2987–3000. [PubMed: 19934022]
6. Buza-Vidas N, et al. GATA3 is redundant for maintenance and self-renewal of hematopoietic stem cells. Blood. 2011; 118:1291–3. [PubMed: 21670475]
7. Ku CJ, Hosoya T, Maillard I, Engel JD. GATA-3 regulates hematopoietic stem cell maintenance and cell cycle entry. Blood. 2012; 119:2242–2251. [PubMed: 22267605]
8. Maneechotesuwan K, et al. Regulation of Th2 cytokine genes by p38 MAPK-mediated phosphorylation of GATA-3. J Immunol. 2007; 178:2491–8. [PubMed: 17277157]
9. Benveniste P, Cantin C, Hyam D, Iscove NN. Hematopoietic stem cells engraft in mice with absolute efficiency. Nat Immunol. 2003; 4:708–13. [PubMed: 12766767]
10. Wilson A, et al. Hematopoietic stem cells reversibly switch from dormancy to self-renewal during homeostasis and repair. Cell. 2008; 135:1118–29. [PubMed: 19062086]

11. Foudi A, et al. Analysis of histone 2B-GFP retention reveals slowly cycling hematopoietic stem cells. Nat Biotechnol. 2009; 27:84–90. Epub 2008 Dec 5. [PubMed: 19060879]
12. Dykstra B, et al. Long-term propagation of distinct hematopoietic differentiation programs in vivo. Cell Stem Cell. 2007; 1:218–229. [PubMed: 18371352]
13. Trumpp A, Essers M, Wilson A. Awakening dormant haematopoietic stem cells. Nat Rev Immunol. 2010; 10:201–9. [PubMed: 20182459]
14. Kiel MJ, et al. SLAM family receptors distinguish hematopoietic stem and progenitor cells and reveal endothelial niches for stem cells. Cell. 2005; 121:1109–21. [PubMed: 15989959]
15. Grote D, Souabni A, Busslinger M, Bouchard M. Pax 2/8-regulated Gata 3 expression is necessary for morphogenesis and guidance of the nephric duct in the developing kidney. Development. 2006; 133:53–61. [PubMed: 16319112]
16. Lange A, et al. Classical nuclear localization signals: definition, function, and interaction with importin alpha. J Biol Chem. 2007; 282:5101–5105. [PubMed: 17170104]
17. Wang Y, Kellner J, Liu L, Zhou D. Inhibition of p38 Mitogen-Activated Protein Kinase Promotes Ex Vivo Hematopoietic Stem Cell Expansion. Stem Cells Dev. 2011
18. Adams JL, et al. Pyrimidinylimidazole inhibitors of CSBP/p38 kinase demonstrating decreased inhibition of hepatic cytochrome P450 enzymes. Bioorg Med Chem Lett. 1998; 8:3111–6. [PubMed: 9873686]
19. Adams JL, et al. Pyrimidinylimidazole inhibitors of p38: cyclic N-1 imidazole substituents enhance p38 kinase inhibition and oral activity. Bioorg Med Chem Lett. 2001; 11:2867–70. [PubMed: 11597418]
20. Boehm JC, et al. Phenoxypyrimidine inhibitors of p38alpha kinase: synthesis and statistical evaluation of the p38 inhibitory potencies of a series of 1-(piperidin-4-yl)-4-(4-fluorophenyl)-5-(2-phenoxypyrimidin-4-yl) imidazoles. Bioorg Med Chem Lett. 2001; 11:1123–6. [PubMed: 11354358]
21. Yamashita M, Chattopadhyay S, Fensterl V, Zhang Y, Sen GC. A TRIF-independent branch of TLR3 signaling. J Immunol. 2012; 188:2825–2833. [PubMed: 22323545]
22. Essers MA, et al. IFNalpha activates dormant haematopoietic stem cells in vivo. Nature. 2009; 458:904–8. [PubMed: 19212321]
23. Sato T, et al. Interferon regulatory factor-2 protects quiescent hematopoietic stem cells from type I interferon-dependent exhaustion. Nat Med. 2009; 15:696–700. [PubMed: 19483695]
24. Grote D, et al. Gata3 acts downstream of beta-catenin signaling to prevent ectopic metanephric kidney induction. PLoS Genet. 2008; 4:e1000316. [PubMed: 19112489]
25. Pawliuk R, Eaves C, Humphries RK. Evidence of both ontogeny and transplant dose-regulated expansion of hematopoietic stem cells in vivo. Blood. 1996; 88:2852–2858. [PubMed: 8874181]
26. Iscove NN, Nawa K. Hematopoietic stem cells expand during serial transplantation in vivo without apparent exhaustion. Current Biology. 1997; 7:805–808. [PubMed: 9368765]
27. Kouros-Mehr H, Slorach EM, Sternlicht MD, Werb Z. GATA-3 maintains the differentiation of the luminal cell fate in the mammary gland. Cell. 2006; 127:1041–55. [PubMed: 17129787]
28. Eeckhoute J, et al. Positive cross-regulatory loop ties GATA-3 to estrogen receptor alpha expression in breast cancer. Cancer Res. 2007; 67:6477–83. [PubMed: 17616709]
29. Kong SL, Li G, Loh SL, Sung WK, Liu ET. Cellular reprogramming by the conjoint action of ERalpha, FOXA1, and GATA3 to a ligand-inducible growth state. Mol Syst Biol. 2011; 7:526. [PubMed: 21878914]
30. Serandour AA, et al. Epigenetic switch involved in activation of pioneer factor FOXA1-dependent enhancers. Genome Res. 2011; 21:555–65. [PubMed: 21233399]
31. Zaret KS, Carroll JS. Pioneer transcription factors: establishing competence for gene expression. Genes Dev. 2011; 25:2227–41. [PubMed: 22056668]
32. Harrison DE, Lerner CP. Most primitive hematopoietic stem cells are stimulated to cycle rapidly after treatment with 5-fluorouracil. Blood. 1991; 78:1237–1240. [PubMed: 1878591]
33. Quesniaux VF, et al. Use of 5-fluorouracil to analyze the effect of macrophage inflammatory protein-1 alpha on long-term reconstituting stem cells in vivo. Blood. 1993; 81:1497–1504. [PubMed: 8453096]

34. Randall TD, Weissman IL. Phenotypic and functional changes induced at the clonal level in hematopoietic stem cells after 5-fluorouracil treatment. Blood. 1997; 89:3596–3606. [PubMed: 9160664]
35. Barone FC, et al. SB 239063, a Second-Generation p38 Mitogen-Activated Protein Kinase Inhibitor, Reduces Brain Injury and Neurological Deficits in Cerebral Focal Ischemia. J Pharmacol Exp Therapeutics. 2001; 296:312–321.
36. Jia YT, et al. Activation of p38 MAPK by reactive oxygen species is essential in a rat model of stress-induced gastric mucosal injury. J Immunol. 2007; 179:7808–19. [PubMed: 18025227]
37. Pisegna S, et al. p38 MAPK activation controls the TLR3-mediated up-regulation of cytotoxicity and cytokine production in human NK cells. Blood. 2004; 104:4157–4164. [PubMed: 15315972]
38. Bohnenkamp HR, Papazisis KT, Burchell JM, Taylor-Papadimitriou J. Synergism of Toll-like receptor-induced interleukin-12p70 secretion by monocyte-derived dendritic cells is mediated through p38 MAPK and lowers the threshold of T-helper cell type 1 responses. Cell Immunol. 2007; 247:72–84. [PubMed: 17927969]
39. Kapur R, Chandra S, Cooper R, McCarthy J, Williams DA. Role of p38 and ERK MAP kinase in proliferation of erythroid progenitors in response to stimulation by soluble and membrane isoforms of stem cell factor. Blood. 2002; 100:1287–93. [PubMed: 12149209]
40. Katsoulidis E, et al. Role of the p38 mitogen-activated protein kinase pathway in cytokine-mediated hematopoietic suppression in myelodysplastic syndromes. Cancer Res. 2005; 65:9029–37. [PubMed: 16204077]
41. Ito K, et al. Reactive oxygen species act through p38 MAPK to limit the lifespan of hematopoietic stem cells. Nat Med. 2006; 12:446–51. [PubMed: 16565722]
42. Trevisan M, Iscove NN. Phenotypic analysis of murine long-term hemopoietic reconstituting cells quantitated competitively in vivo and comparison with more advanced colony-forming progeny. J Exp Med. 1995; 181:93–103. [PubMed: 7807027]
43. Brady G, et al. Analysis of gene expression in a complex differentiation hierarchy by global amplification of cDNA from single cells. Current Biology. 1995; 5:909–922. [PubMed: 7583149]
44. Billia F, Barbara M, McEwen J, Trevisan M, Iscove NN. Resolution of pluripotential intermediates in murine hematopoietic differentiation by global complementary DNA amplification from single cells: confirmation of assignments by expression profiling of cytokine receptor transcripts. Blood. 2001; 97:2257–2268. [PubMed: 11290586]
45. Hardy RR, Carmack CE, Shinton SA, Kemp JD, Hayakawa K. Resolution and characterization of pro-B and pre-pro-B cell stages in normal mouse bone marrow. 1991. J Immunol. 2012; 189:3271–3283. [PubMed: 22997230]
46. Schwarz BA, et al. Selective thymus settling regulated by cytokine and chemokine receptors. J Immunol. 2007; 178:2008–2017. [PubMed: 17277104]
47. Iscove NN, et al. Representation is faithfully preserved in global cDNA amplified exponentially from sub-picogram quantities of mRNA. Nat Biotechnol. 2002; 20:940–943. [PubMed: 12172558]
48. Muro EM, et al. Identification of gene 3′ ends by automated EST cluster analysis. Proc Natl Acad Sci USA. 2008; 105:20286–90. [PubMed: 19095794]

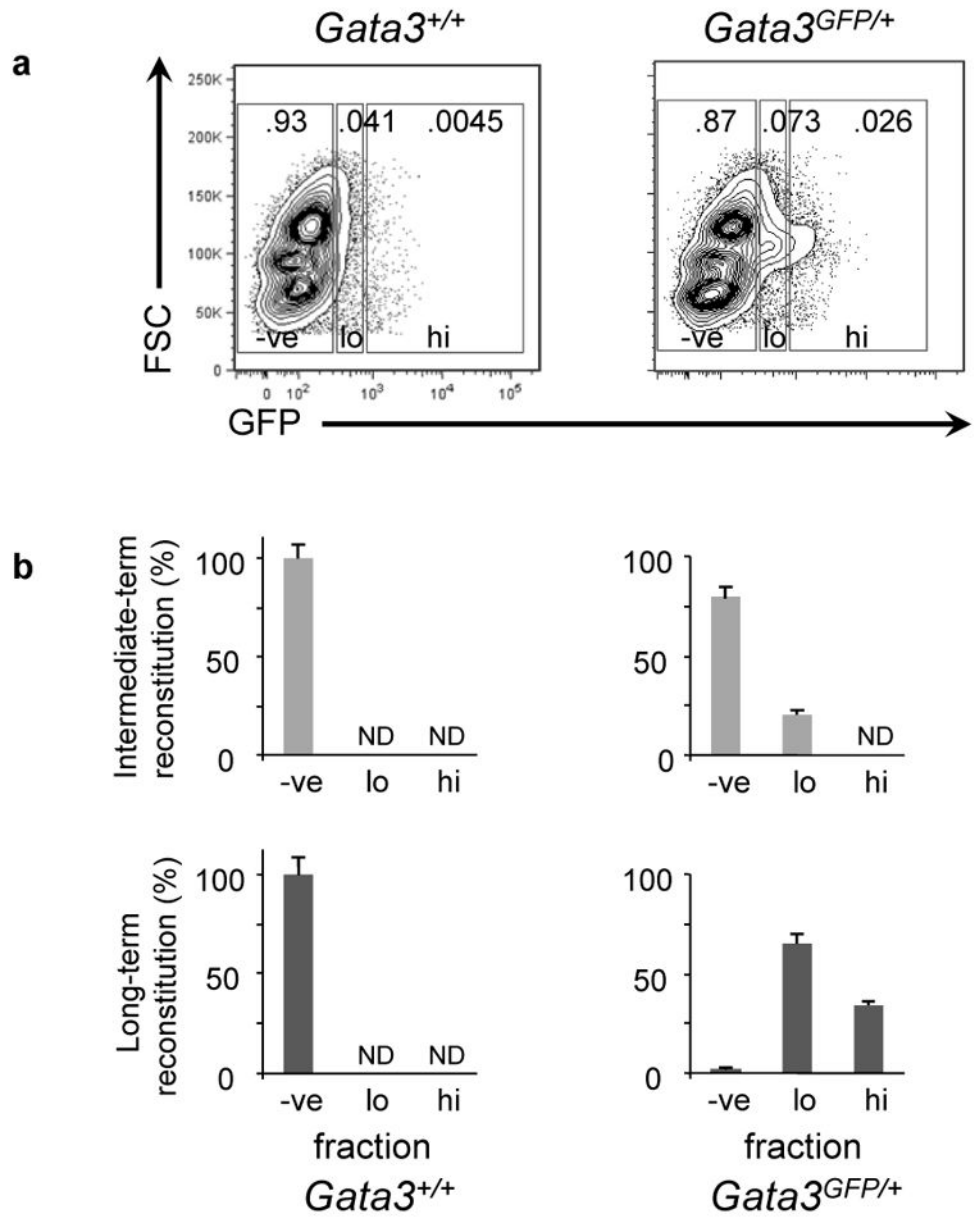

Figure 1. *Gata3* is actively transcribed in LT- but not IT-HSC

(a) GFP fluorescence intensity distributions in bone marrow cells from wild-type or *Gata3*$^{GFP/+}$ mice expressing a GFP cassette under control of the endogenous *Gata3* promoter. Total bone marrow cells were gated on forward and side scattering channels to exclude outliers. (**b**) Erythroid reconstitution from C57BL/6J-*GPI1b-Gata3*$^{+/+}$ (left) or C57BL/6J-*GPI1b-Gata3*$^{GFP/+}$ (right) bone marrow cells fractionated according to eGFP fluorescence and transferred in competition with wild-type cells of host genotype into lethally irradiated C57BL/6J-*GPI1a* mice. Blood samples were analysed at 8 and 32 wk post-transplant (3 mice per fraction in each of 2 independent experiments). Results from both experiments were pooled. The number of 8 wk (intermediate-term, top) and 32 wk (long-term, bottom) erythroid repopulating cells per fraction was calculated. The results for

each fraction were normalized to percentage of total repopulating cells recovered from all 3 fractions. The number of intermediate term cells was the number calculated in a fraction at 8 wk minus the number determined at 32 wk.

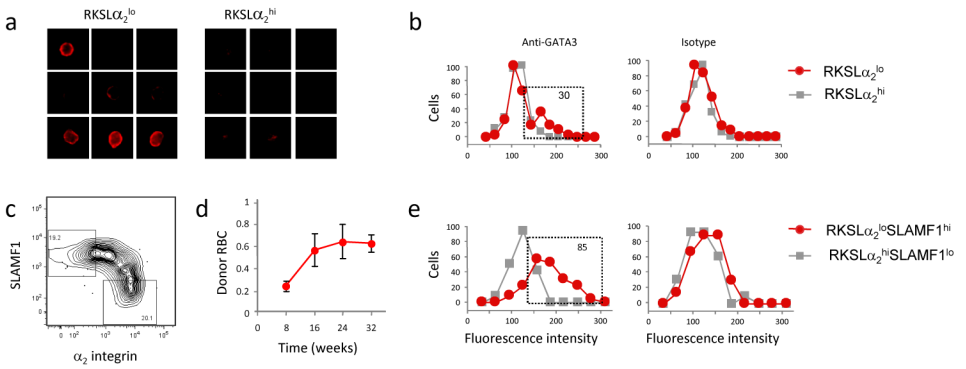

Figure 2. GATA3 protein is expressed in LT- but not IT-HSC

(a) Immonufluorescence analysis of GATA3 expression in LSKRα_2^{lo} and α_2^{hi} cells. LSKRα_2^{lo} and α_2^{hi} cells were sorted, fixed, permeabilized and stained for GATA3. Representative images are shown. GATA3 staining was detected in approximately 1/3 of LSKRα_2^{lo} but not in α_2^{hi} cells. **(b, e)** Quantification of GATA3 flurorescence intensity in purified HSC. Total fluorescence signal was measured in individual cell images stained with mouse anti-GATA3 (left panel) or isotype control (IgG, right panel). Frequencies were normalized to a mode of 100 for α_2^{hi} cell images and equal total areas on each plot. The proportion of cells expressing GATA3 above background was 30% and 85% for LSKRα_2^{lo} and LSKRα_2^{lo}SLAMF1^{hi} cells respectively. Results were aggregated from 5 and 3 independent separations respectively. **(c)** Isolation of LSKR α_2^{lo}SLAMF1^{hi} and α_2^{hi}SLAMF1^{lo} cells. Events shown were gated on LSKR parameters. **(d)** High functional purity of the LSKRα_2^{lo}SLAMF1^{hi} cell fraction. 50 sorted cells were coinjected with 10^6 bone marrow cell competitors of host genotype into lethally irradiated recipients in 2 independent experiments. Historically this competitor dose would contain about 50 LT-HSC [2]. Donor red blood cell reconstitution was measured at 8 wk intervals after transplantation with SEMs indicated. Achievement of 50% donor reconstitution at 24 – 32 wk is indicative of functional homogeneity of the LSKRα_2^{lo}SLAMF1^{hi} fraction.

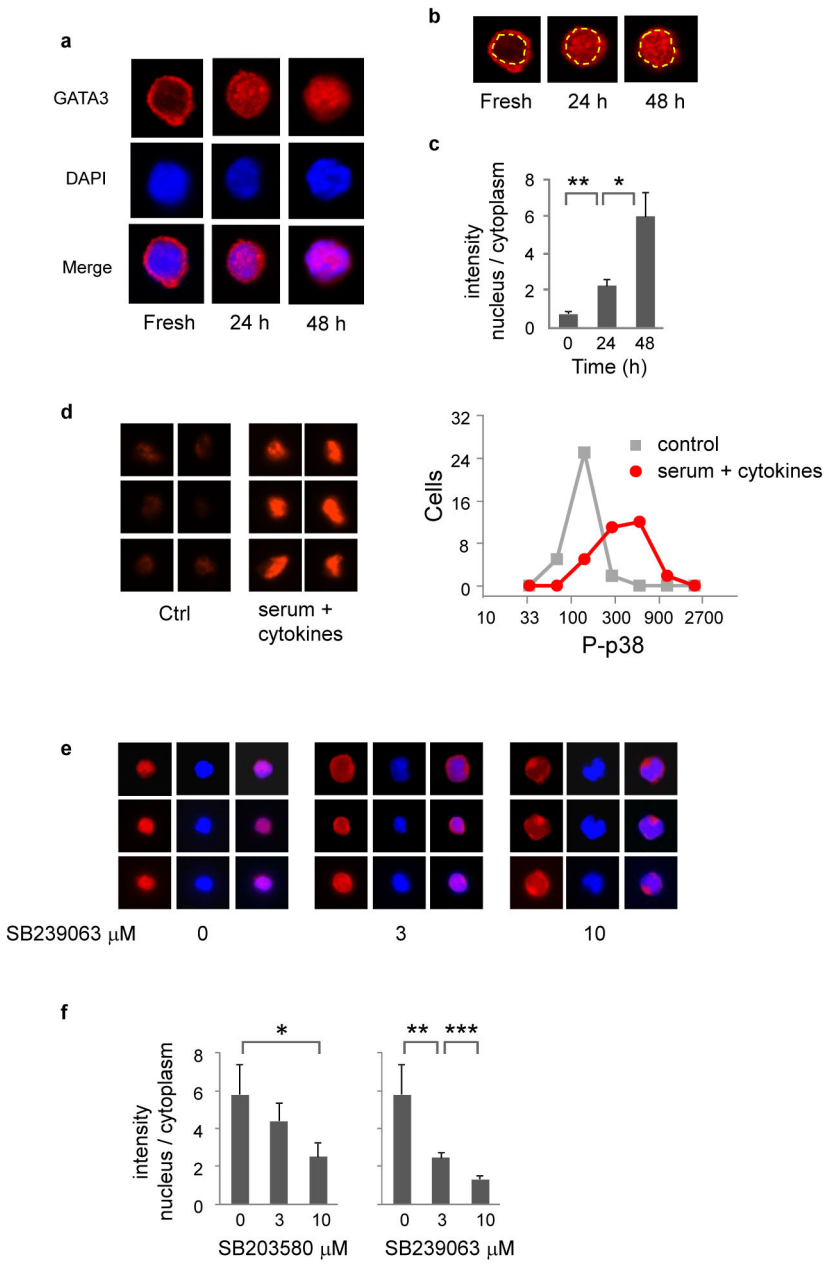

Figure 3. GATA3 relocalizes to the nucleus in cycling cells and the effect is inhibited by p38α inhibitors

(a) Subcellular localisation of GATA3 in quiescent and cultured LT-HSC. LSKRα$_2^{lo}$ cells were stained for GATA3 and DNA counterstained with DAPI, directly after sorting or after culture. **(b,c)** Whole cell and nuclear fluorescence pixel intensities were summed for individual cells in microscopy images. The nuclear perimeter was traced in the DAPI-stained images and duplicated in the GATA3-stained images. The measurements are plotted as the mean ratio of summed nuclear to cytoplasmic fluorescence pixel intensities (n=6 or 7 cells for each value) with SEMs and 1-tail T test probabilities indicated (* = .031; ** = .00026). **(d)** Phospho-p38 MAPK staining in cultured LT-HSC. LSKRα$_2^{lo}$SLAMF1^{hi} cells were

cultured for 1 h in serum- and cytokine-free medium after which serum and cytokines were added. Controls received medium without serum and cytokines. After a further 15 min incubation cells were stained with anti-phospho-p38α antibody. Pixel intensities were summed for individual cells in fluorescence microscopy images. Frequencies were normalized as in figure 2b. Results are aggregated from 3 independent experiments. **(e)** Effect of p38α inhibitors. LSKRα_2^{lo}SLAMF1^{hi} cells were cultured for 2 d with cytokines and SB239063 prior to staining and assessment of GATA3 localization by confocal microscopy. **(f)** Quantitation of GATA3 fluorescence localization in the presence of p38α inhibitors. Means + SEM from 2 independent experiments are shown with 1-tail T test probabilities (* = .026; ** = .00090, *** = 4.4E-04).

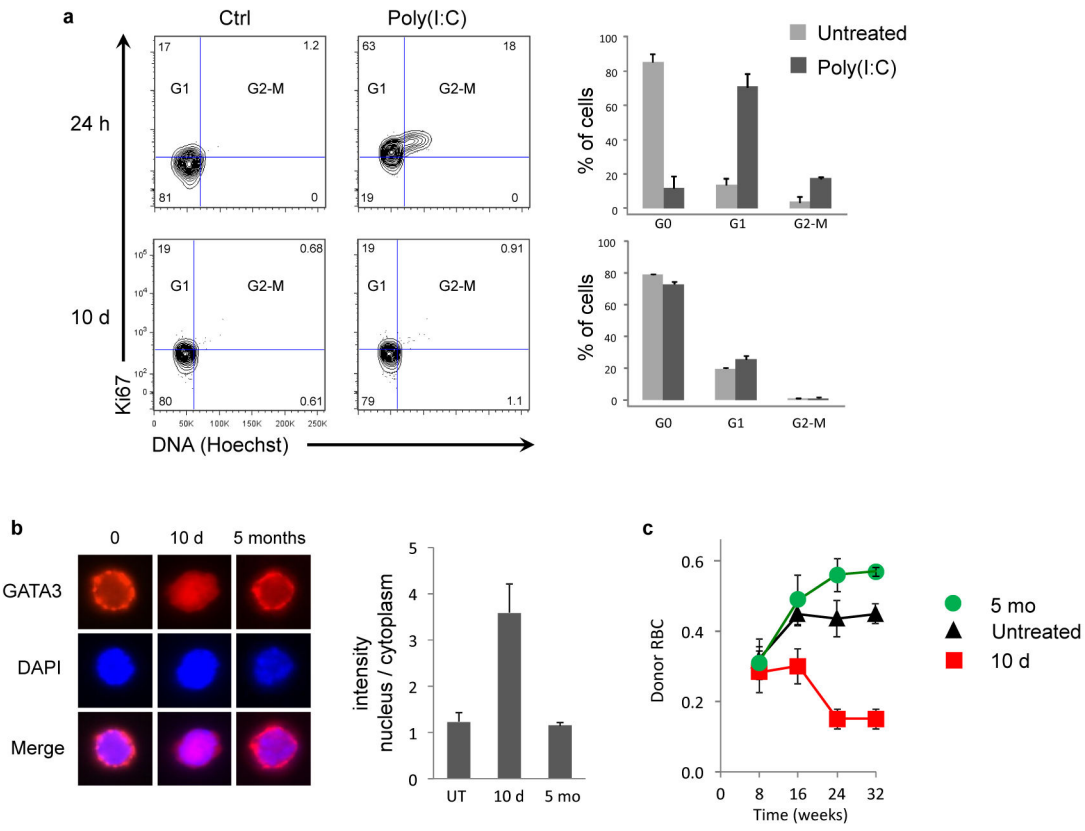

Figure 4. Poly(I:C) treatment induces HSC cycling and GATA3 relocalization in vivo and reduces the long-term reconstituting capacity of LSKRα$_2^{lo}$ cells

(a) Cell cycle analysis in LSKα$_2^{lo}$SLAMF1^{hi} cells at 1 and 10 d after in vivo treatment with poly(I:C). Cells were stained with anti-human Ki67 and Hoechst 33342 and analyzed by flow cytometry (left). Cycle phase distributions are plotted (right) showing means + SEM of 2 independent experiments. **(b)** Subcellular localization of GATA3 in LSKRα$_2^{lo}$ cells after poly(I:C) treatment analysed by confocal microscopy. Whole cell and nuclear fluorescence intensities were summed in images of individual GATA3-positive cells (n=6 for each condition). The ratios of nuclear to cytoplasmic intensities are plotted (right) showing means + SEM. UT = Untreated. **(c)** 100 LSKRα$_2^{lo}$ cells from control or poly(I:C) treated mice were injected in competition with 10^6 bone marrow cells of host genotype into lethally irradiated recipients and erythroid reconstitution was tracked. Means and SEMs from 5 independent experiments are plotted.

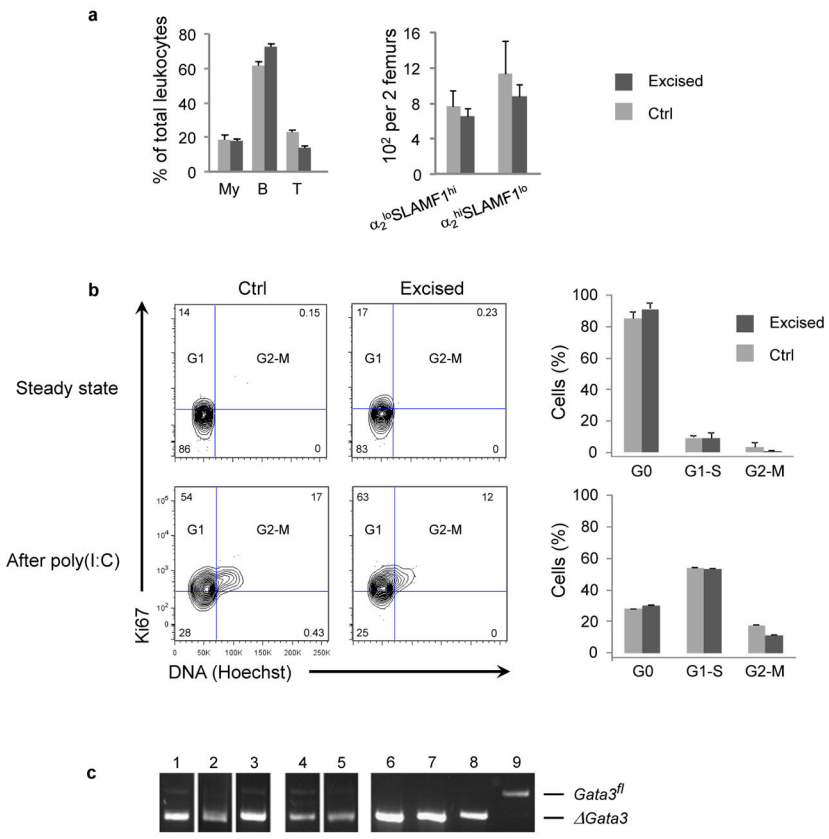

Figure 5. *Gata3* excision has little effect on steady state bone marrow and blood populations

Gata3$^{fl/f}$ ("Control") or *Gata3*$^{fl/fl}$-*Mx1-Cre* ("Excised") mice were treated with poly(I:C) and analyzed 3 – 9 months later ("steady state"). **(a)** Myeloid and lymphoid cells (proportion of total cells, n=7 independent experiments) in blood and absolute numbers of phenotypic LT- and IT-HSC (n=4 and 3) in steady state bone marrow. **(b)** Cell cycle analysis in LSKα_2^{lo}SLAMF1^{hi} bone marrow cells in steady state bone marrow or 1 d after a new poly(I:C) treatment. The bar graphs show means + SEM of 2 independent experiments. **(c)** Representative PCR reactions on DNA for assessment of *Gata3* excision at the indicated times after treatment with poly(I:C). Image contrast and gamma were adjusted to allow visualization of the faint *Gata3*^{fl} band. 1, bone marrow 2 wk; 2, bone marrow 8 wk; 3, bone marrow 24 wk; 4, blood myeloid 7 mo; 5, blood myeloid 10 mo; 6–8, LSKR clones 10 d after excision; 9, *Gata3*$^{fl/fl}$ unexcised control.

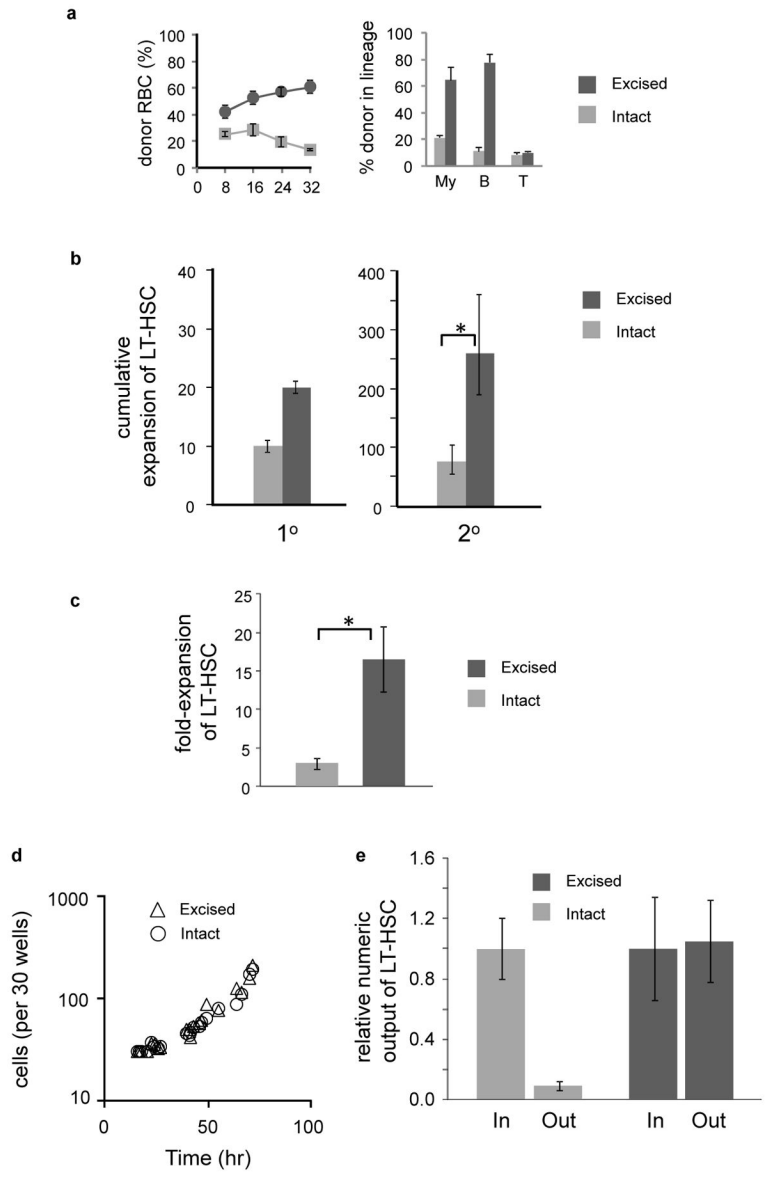

Figure 6. Regenerative activity and self-renewal are enhanced in vivo and in vitro after *Gata3* deletion

(a) *Gata3*$^{fl/fl}$-*Mx1-Cre* ("excised") and control *Gata3*$^{fl/fl}$ ("intact") mice were treated with poly(I:C). 10^6 marrow cells taken 10 d later were injected with 10^6 host-genotype bone marrow cells into irradiated recipients. Donor red cells were measured at intervals post-transplant (left). Proportions of donor myeloid and lymphoid cells in blood were measured at 32 wk (right). Means and SEMs of 3 independent experiments are indicated. **(b)** *Gata3*-deleted bone marrow cells were transplanted into irradiated 1° recipients with normal competitors. After 24 wk, bone marrow was transfered to irradiated 2° recipients. The bar graphs show the cumulative fold-expansion in LT-HSC numbers in 1° and 2° recipients with SEMs and 1-tail T test probabilities indicated. **(c)** *Gata3*$^{fl/fl}$ or *Gata3*$^{fl/fl}$-*Mx1-Cre*] bone marrow cells were injected with normal competitors into irradiated wild type recipients. Hosts were treated with poly(I:C) 8 wk later. At 24 wk, bone marrow cells were assayed

competitively in vivo for long-term erythroid reconstituting activity. The bar graph shows the fold-expansion in LT-HSC numbers calculated to have occurred in the 1° recipients with SEMs indicated (single experiment, 3 – 5 mice per point, * = .04, 1-tail T test). **(d)** Bone marrow from *Gata3*$^{fl/fl}$-*Mx1-Cre*] and control *Gata3*$^{fl/fl}$ mice was analyzed 2–3 months after treatment with poly(I:C). Single LSKRα_2^{lo} (n=3 independent experiments) or LSKRα_2^{lo}SLAMF1^{hi} (n=1) cells were cultured per well with serum and cytokines, and cell numbers were recorded every 4–8 hr. Each point represents the sum of cells in 30 wells. **(e)** LSKRα_2^{lo}SLAMF1^{hi} cells, 25, from *Gata3*$^{fl/fl}$-*Mx1-Cre* or control *Gata3*$^{fl/fl}$ mice treated 3 – 5 months earlier with poly(I:C) were cultured at 1 per well, and also assayed competitively in vivo for long-term erythroid reconstitution. After 7 d all harvested cells were again assayed in vivo. The bar graph shows SEM and mean relative number of LT-HSC recovered from 7 d cultures (“Out”) relative to the number initiating the cultures (“In”) in 2 independent experiments.